COMPUTATIONAL PREDICTION OF PH-DEPENDENT BINDING ENERGIES IN HPV CAPSID ANTIBODY INTERACTIONS

By

Amjad Alqarni

APPROVED:

Graduate Committee:

_____

Supervisor Dr. Joshua L. Phillips (Computer Science)

_____

Dr. Cen Li (Computer Science)

_____

Dr. Yi Gu (Computer Science)

_____

Dr. Medha Sarkar, Chairperson Computer Science Department

_____

Dr. David Butler, Dean of the College of Graduate Studies

Computational Prediction of pH-Dependent Binding Energies in HPV Capsid Antibody Interactions

By

Amjad Alqarni

A thesis submitted in partial fulfillment

of the requirements for the degree of

MASTER OF SCIENCE

in

Computer Science

Middle Tennessee State University

(May 2023)

Thesis Committee:

Dr. Joshua L. Phillips

Dr. Cen Li

Dr. Yi Gu

I dedicate this thesis to my parents for their unconditional love, boundless patience, endless support, and belief in me to achieve anything.

ACKNOWLEDGEMENTS

I would like to thank my great advisor, Dr. Joshua Phillips, who guided me through the process of this work and directed me to this field, and without him I would not have completed this work, as he is the one who taught me and explained to me everything related to this work. Also, he taught me the basics of research, and I am honored to have been taught by him. Also, I would like to thank my committee members Dr. Cen Li and Dr. Yi Gu. Most importantly, I would like to express my sincerest gratitude to my parents for always being there for me, for motivating me to reach my full potential, and for being my constant source of inspiration. I am truly blessed to have you as my parent. I would also like to express my deepest gratitude to my siblings, who have been my pillars of strength and have always stood by my side. Words cannot express my gratitude to my husband for his unwavering love and support throughout this journey.

ABSTRACT

HPV is the most common sexually transmitted infection in the world. In high-risk types, HPV infection is associated with virtually all cervical cancers and a significant proportion of anogenital and oropharyngeal cancers. Neutralizing antibodies can prevent HPV infection with their effectiveness depending on the way they interact with HPV capsid proteins. The ability of antibodies to attach to capsid proteins is influenced by pH variations, which can impact the characteristics and stability of both the viral capsid and the antibody. In this thesis, we apply a computational simulation pipeline to predict the pH-dependent binding energies in HPV capsid-antibody interactions. Our results predict that there is a strong preference for binding to antibody 28F10 for HPV subtypes 6, 16, 18, 33, and 58 while A12A3 shows a strong preference for HPV 35 and 59. The results also predict that both antibodies bind non-preferentially to the HPV 11 capsid.

TABLE OF CONTENTS

LIST OF TABLES

LIST OF FIGURES

LIST OF SYMBOLS AND ABBREVIATIONS

HPV – Human Papillomavirus

PPI – Protein-Protein Interaction

VLP – Virus-Like Particle

VMD – Visual Molecular Dynamics

APBS – Adaptive Poisson-Boltzmann Solver

PDB – Protein Data Bank

pH – Potential Hydrogen

DNA – Deoxyribonucleic Acid

CHAPTER I

INTRODUCTION

Despite the fact that viruses are extremely tiny biological particles, they can have a significant impact on human health and well-being [35]. Human papillomavirus (HPV) is a small double-stranded DNA virus that has over 200 variants and is a common sexually transmitted virus [2]. HPV is associated with various types of cancer, specifically cervical cancer (Figure 1) [34]. One of the challenges facing the world concerning HPV is that there is still no effective treatment for it [6]. Although there are vaccines available to protect against HPV, they offer limited protection against only specific types of the virus, typically up to nine, and are most effective when administered within a specific age range [36].

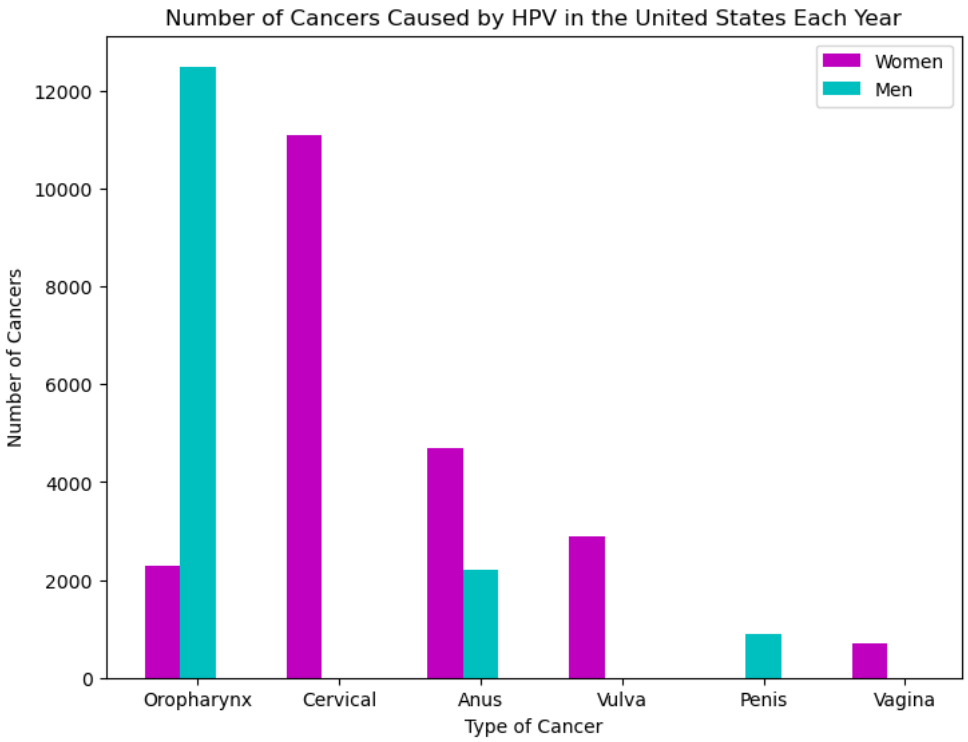

Figure 1. This chart shows the number of cancers caused by HPV in the United States each year.

In the past, the knowledge to analyze protein-protein interactions was limited. Due to the early stages of molecular biology during that time, methods for studying protein-protein interactions and the development of techniques have emerged at a slow pace [37]. However, with the advent of computational methods, they have become a topic of great interest in bioinformatics because they provide the ability to predict protein-protein interactions and validate experimental outcomes [38]. Research in protein-protein interaction (PPIs) has become more efficient using computational methods leading to new ideas and proposals [39]. These developments have contributed significantly to the invention and development of treatments and vaccines, particularly in the study of viruses [40].

This thesis aims to investigate the interactions between each of two antibodies and the capsid protein of several HPV variants/types. The study will predict the binding energy of both antibodies to each type of HPV across pH levels and compare their efficacy in protecting against each type of HPV.

CHAPTER II

BACKGROUND

In this chapter, we introduce related topics to this project to give more information for better understanding of this study. It starts with HPV, HPV vaccines, the structure of HPV, and the pipeline that is applied to this work.

Human Papillomavirus

Human papillomavirus (HPV) is the most common sexually transmitted infection (STI). HPV can affect more than 300,000 people per year worldwide. HPV can not only affect women, but it can also affect men. It is a virus that causes diseases that vary from minor like warts to a high level of disease risk like cancer [1].

HPV has more than 200 types, it is grouped into low-risk types and high-risk types. Low risk types do not cause disease in most cases, but it may cause warts in some parts of the body like the genitals, anus, mouth, or throat. On the other hand, high-risk types can be the main cause of various cancers specifically cervical cancer. High-risk types encompass around 14 types which are: 16, 18, 31, 33, 35, 39, 45, 51, 52, 56, 58, 59, 66, and 68, but 16 and 18 are the most dangerous types that cause cancers. [2]

HPV can transmit through skin to skin contact as well as sexual contact like vaginal, anal, or oral sex [1]. There is a small possibility for the transmission of HPV from the mother to her newborn during childbirth [3]. HPV typically does not manifest with overt symptoms, and many carriers remain unaware of their infection [1]. In instances of low-risk HPV types, skin and genital warts may develop [2]. In women, the presence of HPV is often detected through routine pap smear screenings, which may reveal abnormal cells and frequently test positive for high-risk HPV strains [4]. HPV can lie dormant for

prolonged periods of time unless there are obvious signs such as genital warts [5]. Also, HPV is associated with multiple cancers, not only causing cervical cancer but also cancer of the vulva, vagina, penis, anus, and oropharynx [2].

HPV mostly can go away on its own within two years without health problems for every 9 out of 10 people [1]. At present, there is no real cure for HPV, but there are treatment methods to relieve symptoms resulting from the virus [6]. Surgical removal or topical medications can be used to treat warts, like cryotherapy (freezing) and electrocautery (burning) [7]. Cancer that is caused by HPV typically necessitates treatment with a combination of surgery, radiation, and chemotherapy [8].

Consideration of the pH range over which HPV is likely to be stable and infectious is important when comparing binding energies across different pH values. Focusing on HPV associated with cervical cancer, HPV is primarily transmitted through the cervical and vaginal tract. The relevant pH range may be the pH of the cervical tract which ranges from 6.5 to 7.5 while pH of the vaginal tract is from 3.3 to 4.5 [41].

HPV Vaccines

Vaccines can prevent certain types of HPV infections. There are three types of HPV vaccines that can prevent infection: Cervarix, Gardasil, and Gardasil 9 [9]. Cervarix was authorized for use in the United States in October of 2009 [10]. It protects against only HPV 16 and 18 from age 9 to 25 years old with two doses [11] [12]. For Gardasil, the initial approval of use was in 2006. It is used for ages 9 to 26 years old with three doses. It can prevent four types of HPV which are HPV 6, HPV 11, HPV 16, and HPV 18 [13]. Finally, Gardasil 9 was approved in the Unites States in 2014 [14]. It can protect against nine types

of HPV which are 6, 11, 16, 18, 31, 33, 45, 52, 58 [15]. It is used at the age from 9 to 45 years old [16] (Table 1). Cervarix and Gardasil are no longer be sold in the United States.

Table 1. Summary of all vaccines of HPV.

Vaccine	HPV types protected	Age	Year of Use
Cervarix	16 and 18	9 - 25	2009
Gardasil	6, 11, 16, and 18	9 - 26	2006
Gardasil 9	6, 11, 16, 18, 31, 33, 45, 52, and 58	9 - 45	2014

The Structure of HPV

HPV is a small, non-enveloped virus and has an estimated size of around 55 nm in diameter. The virus consists of a viral genome, a capsid, and some small proteins that play a role in viral replication and assembly [17] (Figure 2). The capsid is formed by the major structural protein, L1, which self-assembles into a non-enveloped icosahedral shell, as well as the minor capsid protein L2 [17] [18]. The L1 protein of HPV is highly immunogenic and has been used in the development of HPV vaccines [19]. Virus-like particles (VLPs) composed of L1 protein have been shown to be highly effective in eliciting an immune response and providing protection against HPV infection [20].

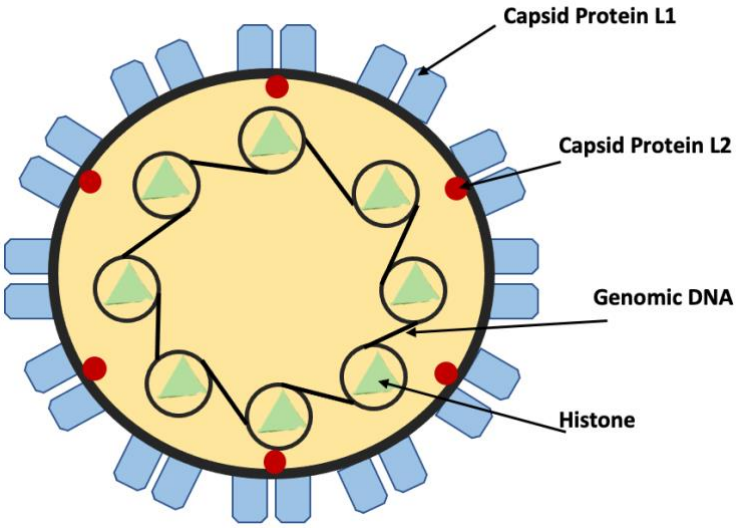

Figure 2. This figure shows the structure of HPV and the components of the virus.

HPV also contains minor proteins that play a role in viral replication and assembly, including E1, E2, E4, E5, E6, and E7. These proteins are involved in viral DNA replication, regulation of gene expression, and interference with host cell function [17].

Pipeline

VMD, Modeller, FrodaN, PDB2PQR, and APBS are common tools in computational biophysics and bioinformatics. Visual molecular dynamics (VMD) is a program for molecular graphics intended for the analysis and presentation of molecular complexes, primarily biopolymers including proteins and nucleic acids. VMD has the capacity to present multiple structures simultaneously, with a diverse range of rendering styles and coloring techniques available [21]. Modeller is a software tool that generates three-dimensional protein structures based on the amino acid sequence and/or a related protein [22]. FrodaN is a bioinformatics tool that can perform docking and shifting of the initial model into the target model [23]. PDB2PQR is a software utility that converts protein

structures that are in the Protein Data Bank (PDB) format into input files that can be used for Poisson-Boltzmann electrostatics calculations [24] [25]. Adaptive Poisson-Boltzmann Solver (APBS) is a software application for calculating the electrostatic properties of biomolecules using the Poisson-Boltzmann equation [26].

CHAPTER III

METHODS

The Template of Capsid, Antibody, and Complex

5Y9C [27] and 5Y9F [27] crystal structures from Protein Data Bank (PDB) [28] were used as complex templates to perform all the simulations. 5Y9C was used for the capsid-antibody A12A3 and 5Y9F was used for the capsid-antibody 28F10.

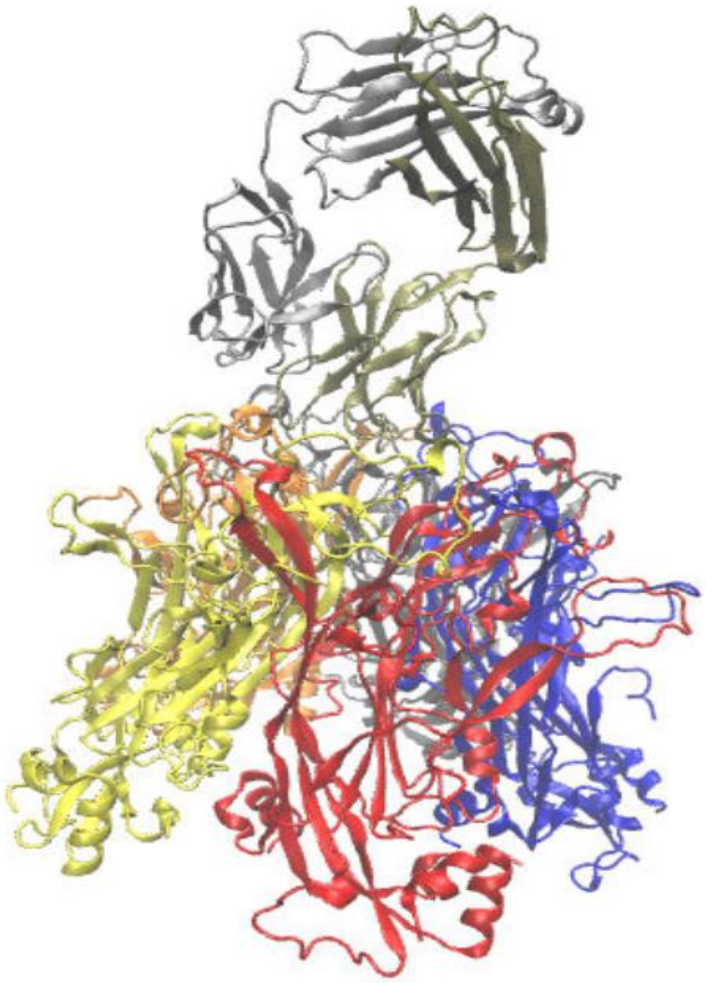

Figure 3. Crystal structure of 5Y9C, with Capsid L1 chains A B C D E and the antibody A12A3 has light chains H and heavy chains L.

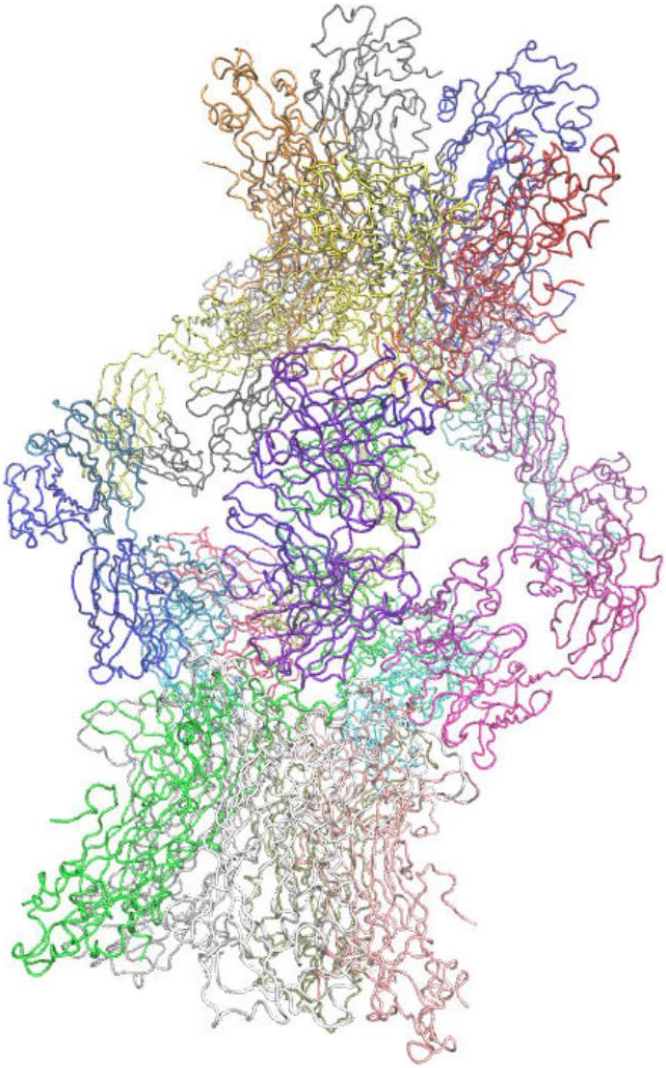

Figure 4. Crystal structure of 28F10 with Capsid L1 chains A B C D E F G H I J and the antibody 28F10 has light chains K M O Q S U W Y a c and heavy chains L N P R T V X Z b.

VMD [21] was used to split both the 5Y9C and 5Y9F crystal structure into a structure of capsid, antibody, and complex by selecting the specific chains for each one as well producing the capsid and antibody apart from one-another.

Generating the Models

For building a model of a capsid protein and the antibody, using the template in the previous step and the sequences, preparation of modeling requirements was performed as follows. First, retrieving the sequences of the capsid protein and the antibody from the Protein Data Bank (PDB) [28] in FASTA format. These sequences serve as the basis for building the models. Creating sequence-only files to make those files used as input for the processing of sequences using a sequence processing script for both the capsid and the antibody. Alignment files for each sequence were obtained by processing them with Modeller. The chain identifiers were modified by updating them in the alignment files to match the corresponding chain identifiers in the template structures. This ensures that the correct chains are used for modeling both capsid and antibody.

Links to the template PDB files were made to be used as a basis for the modeling. This step simplifies the file management and makes it easier to reference the templates during the modeling process by Modeller [22]. Finally, running a Modeller script performed the modeling and generated models using the processed sequences and the template structures. The s-align tool was executed to align the capsid of the HPV variant structure to the same location as the HPV's capsid template. Also, the same pattern was performed with both antibodies to make the model of the antibody aligned in the location of the antibody template producing new aligned models.

Model Docking Approach

The new aligned models of both capsid and antibody were concatenated to be used by FrodaN [23]. The concatenated model was prepared for FrodaN as an initial model, while the template of the capsid-antibody complex was used as a target model. In this step, FrodaN ensures to make the capsid and antibody docked and fit together to form a stable complex.

Binding Energy

Converting PDB models to PQR format by PDB2PQR [24] is required to determine the binding energy. PDB2PQR ensures that PQR models contain the necessary information for calculating the electrical interaction. PQR files of capsid, antibody, and complex were produced across the evaluated pH values. Also, the concatenated file was converted to PQR format to apply the psize tool to it. Psize can determine the finite element grid needed for performing the APBS calculation [26]. APBS was executed to calculate the binding energy across all evaluated pH values. The binding energy was calculated by computing the difference between the electrostatic energy of the capsid-antibody complex and the sum of the individual electrostatic energies of the capsid and the antibody for each specific pH value which are (3.0, 3.5, 4.0, 4.5, 5.0, 5.5, 6.0, 6.5, 7.0, 7.5, 8.0, 8.5, and 9.0).

Data Analysis Protocol

All figures in the results chapter show the plot of binding energy. The plotting was created to represent the data. Each binding energy datapoint was visualized as a circle marker and solid line. Python [32] with its visualization library Matplotlib [33] was used

to represent the data analysis. The plot function was used to draw markers and a line from point to point in the graphs.

HPV Capsid Models

The protocols above were used for all HPV variants by using the specific crystal structure from the PDB for each HPV variant, but utilizing the same files for both antibodies when we make the interaction for the HPV variants.

6L31 [42] was used as the structure of HPV 6 capsid L1 (Figure 5). 2R5K [29] was used as the structure of HPV 11 capsid L1 (Figure 6). 2R5H [29] was used as the structure of HPV 16 capsid L1 (Figure 7). 2R5I [29] was used as the structure of HPV 18 capsid L1 (Figure 8). 6IGE [30] was used as the structure of HPV 33 capsid L1 (Figure 9). 2R5J [29] was used as the structure of HPV 35 capsid L1 (Figure 10). 5Y9E [27] was used as the structure of HPV 58 capsid L1 (Figure 11). 5J6R [31] was used as the structure of HPV 59 capsid L1 (Figure 12).

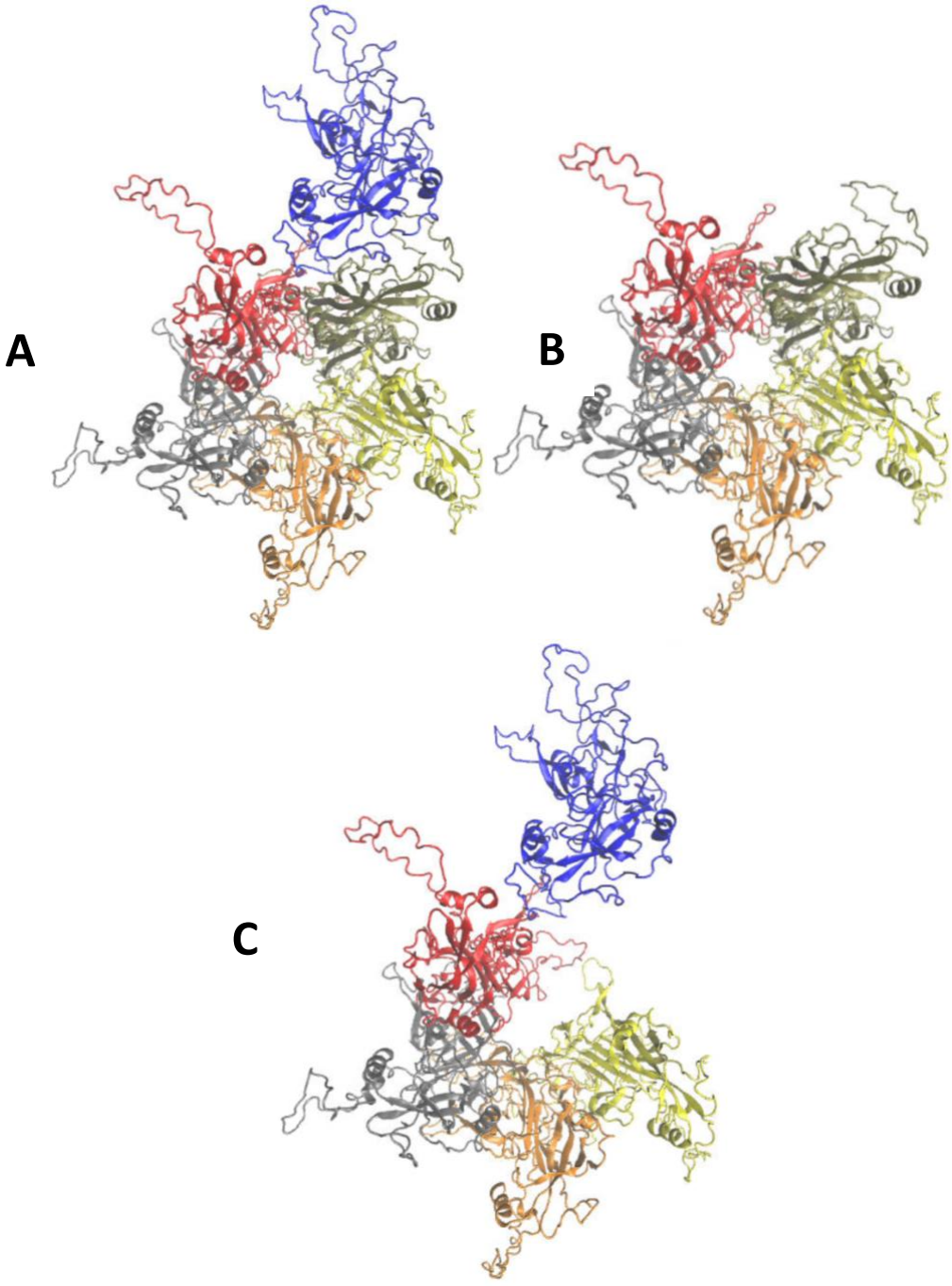

Figure 5. Crystal structure 6L31 of HPV 6 capsid L1 with chains A, B, C, D, E, and F, which was before [Figure 5.A] and after [Figure 5.B] using VMD to choose the only chains B, C, D, E, and F. If A was chosen instead of F the crystal structure would be like in [Figure 5.C].

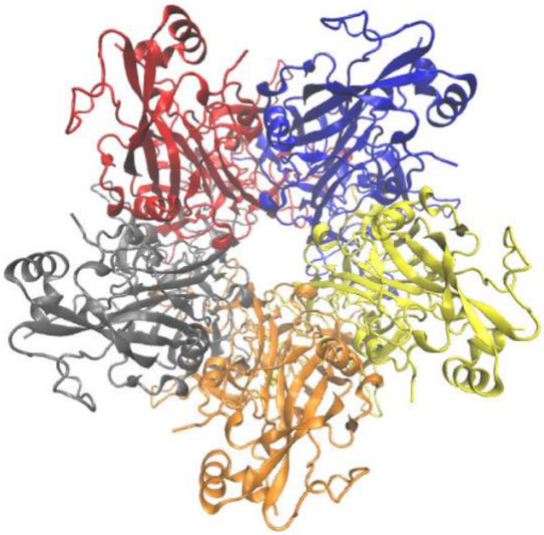

Figure 6. Crystal structure 2R5K of HPV 11 capsid L1 with chains A B C D E.

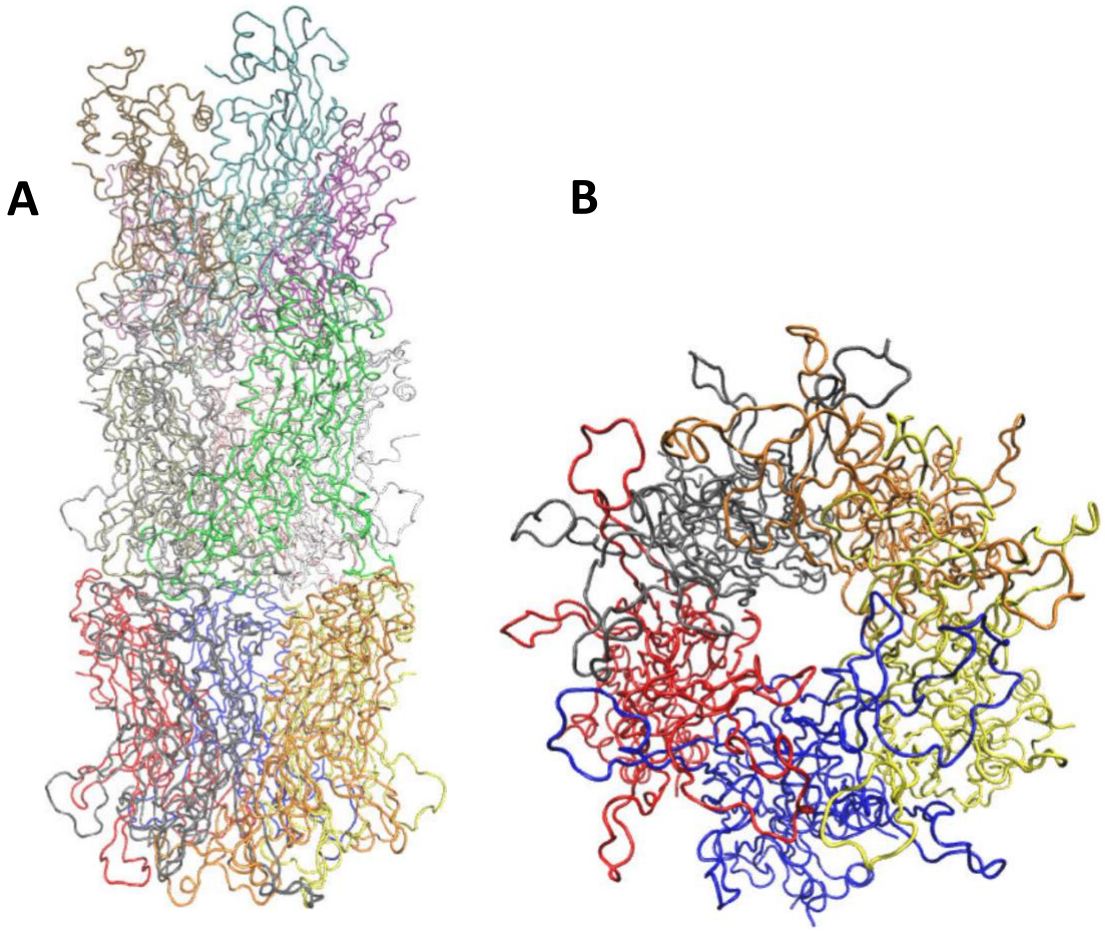

Figure 7. Crystal structure 2R5H of HPV 16 capsid L1 with chains A, B, C, D, E, F, G, H, I, J, K, L, M, N, and O, which was before [Figure 7.A] and after [Figure 7.B] using VMD to choose the only chains A, B, C, D, and E.

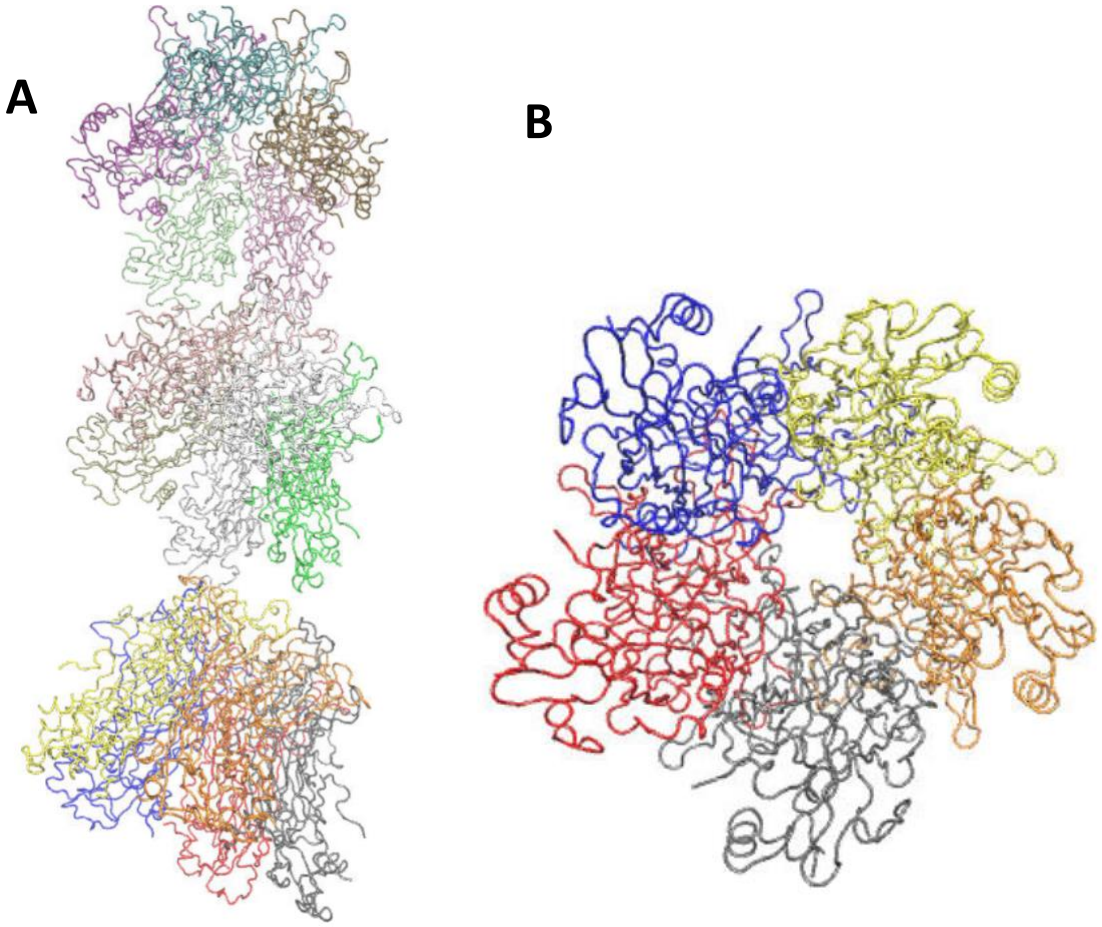

Figure 8. Crystal structure 2R5I of HPV 18 capsid L1 with chains A, B, C, D, E, F, G, H, I, J, K, L, M, N, and O, which was before [Figure 8.A] and after [Figure 8.B] using VMD to choose the only chains A, B, C, D, and E.

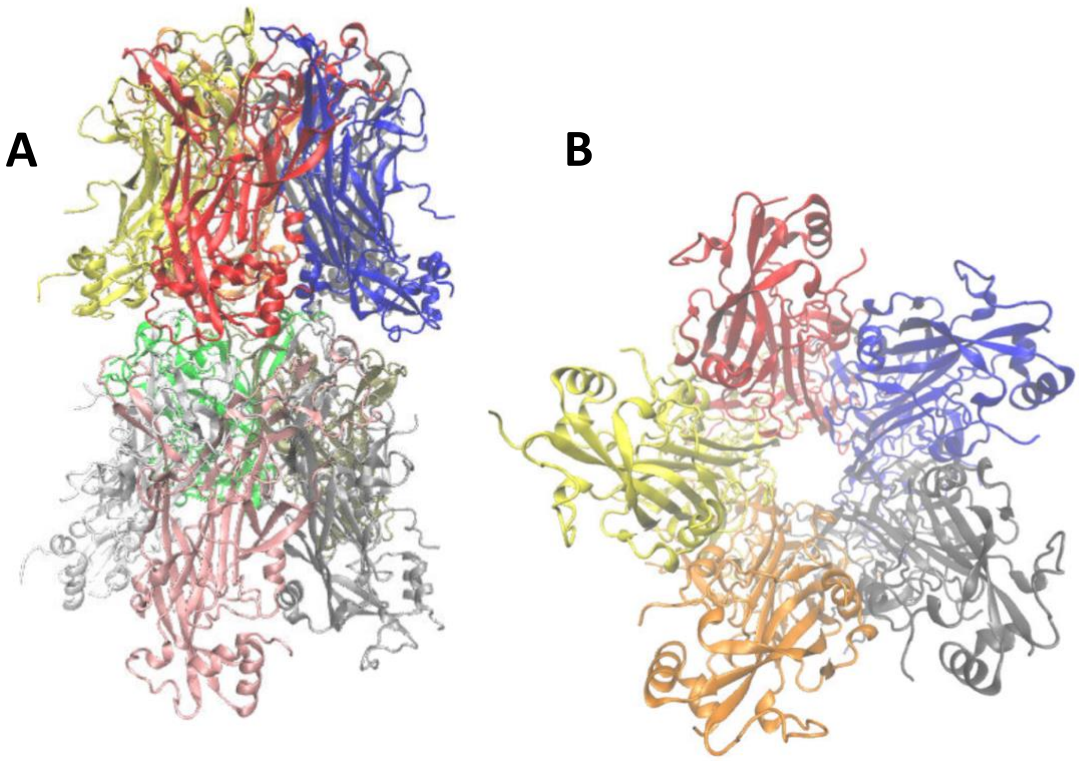

Figure 9. Crystal structure 6IGE of HPV 33 capsid L1 with chains A, B, C, D, E, F, G, H, I, and J, which was before [Figure 9.A] and after [Figure 9.B] using VMD to choose the only chains A, B, C, D, and E.

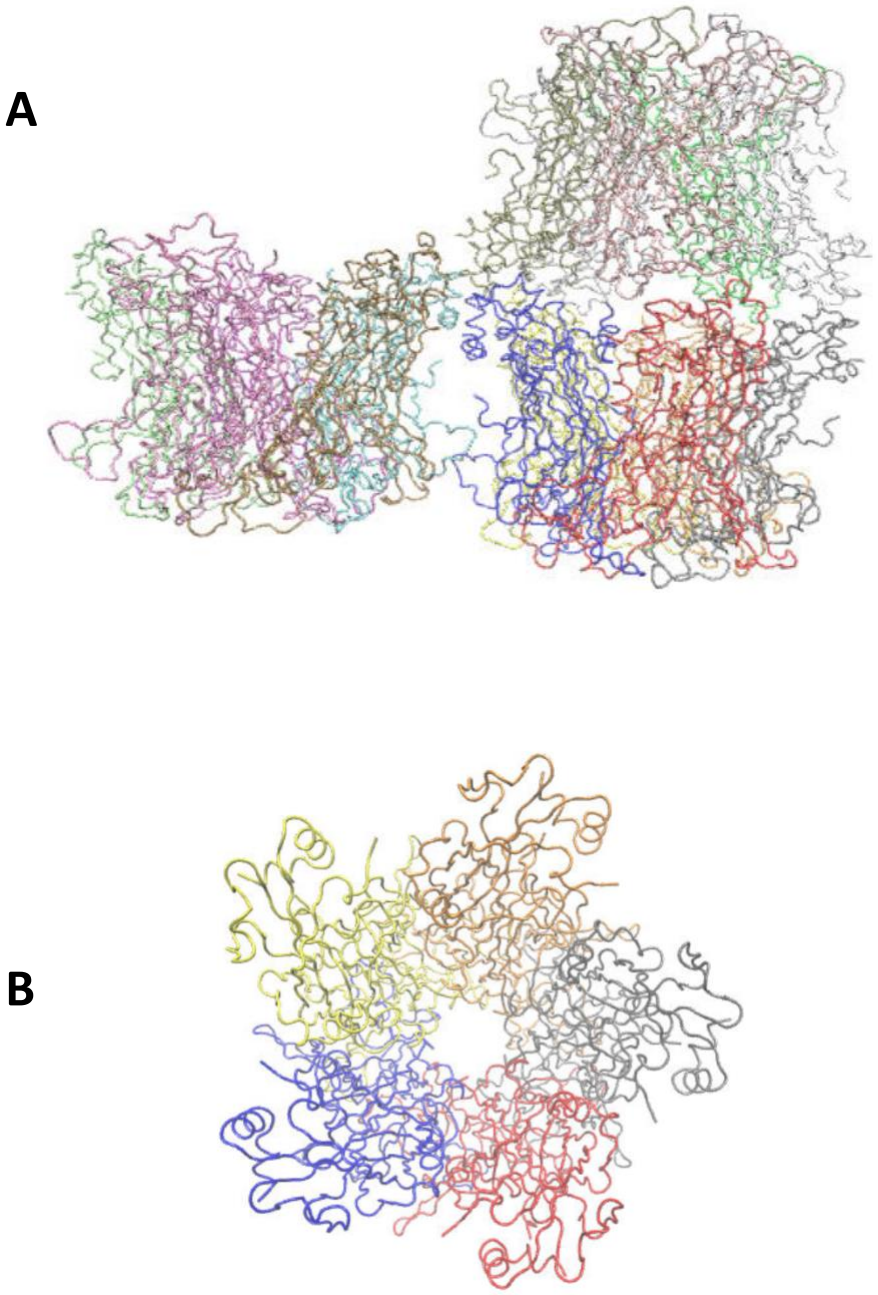

Figure 10. Crystal structure 2R5J of HPV 35 capsid L1 with chains A, B, C, D, E, F, G, H, I, J, K, L, M, N, and O, which was before [Figure 10.A] and after [Figure 10.B] using VMD to choose only the chains A, B, C, D, and E.

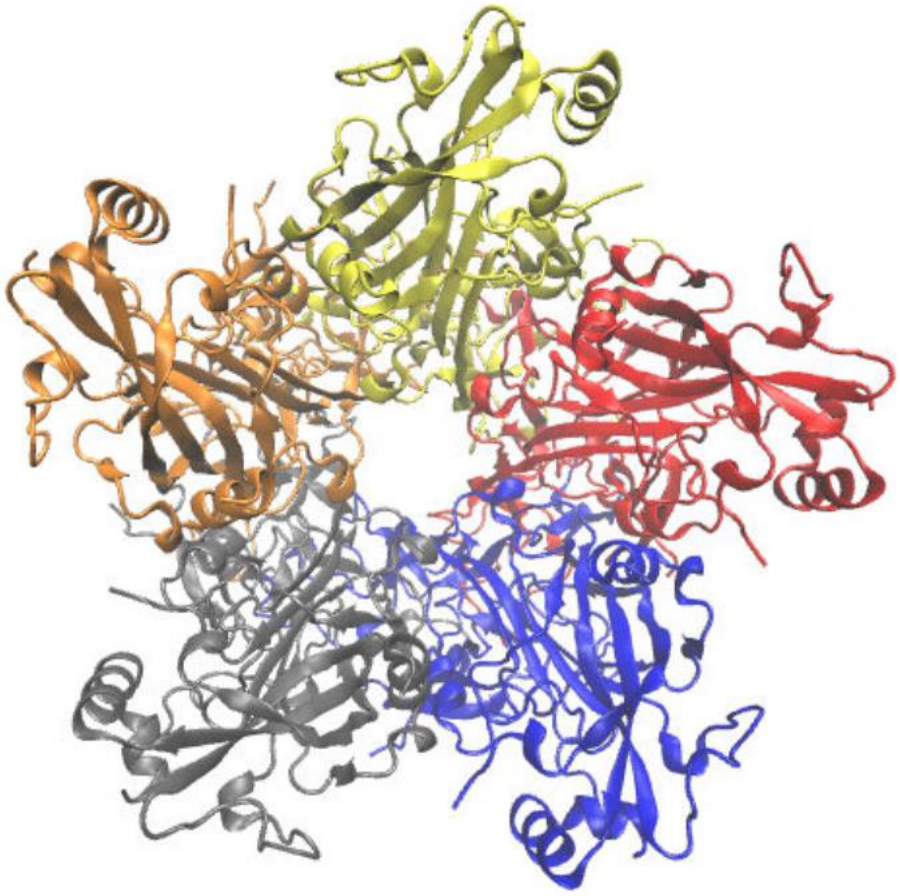

Figure 11. Crystal structure 5Y9E of HPV 58 capsid L1 with chains A B C D E.

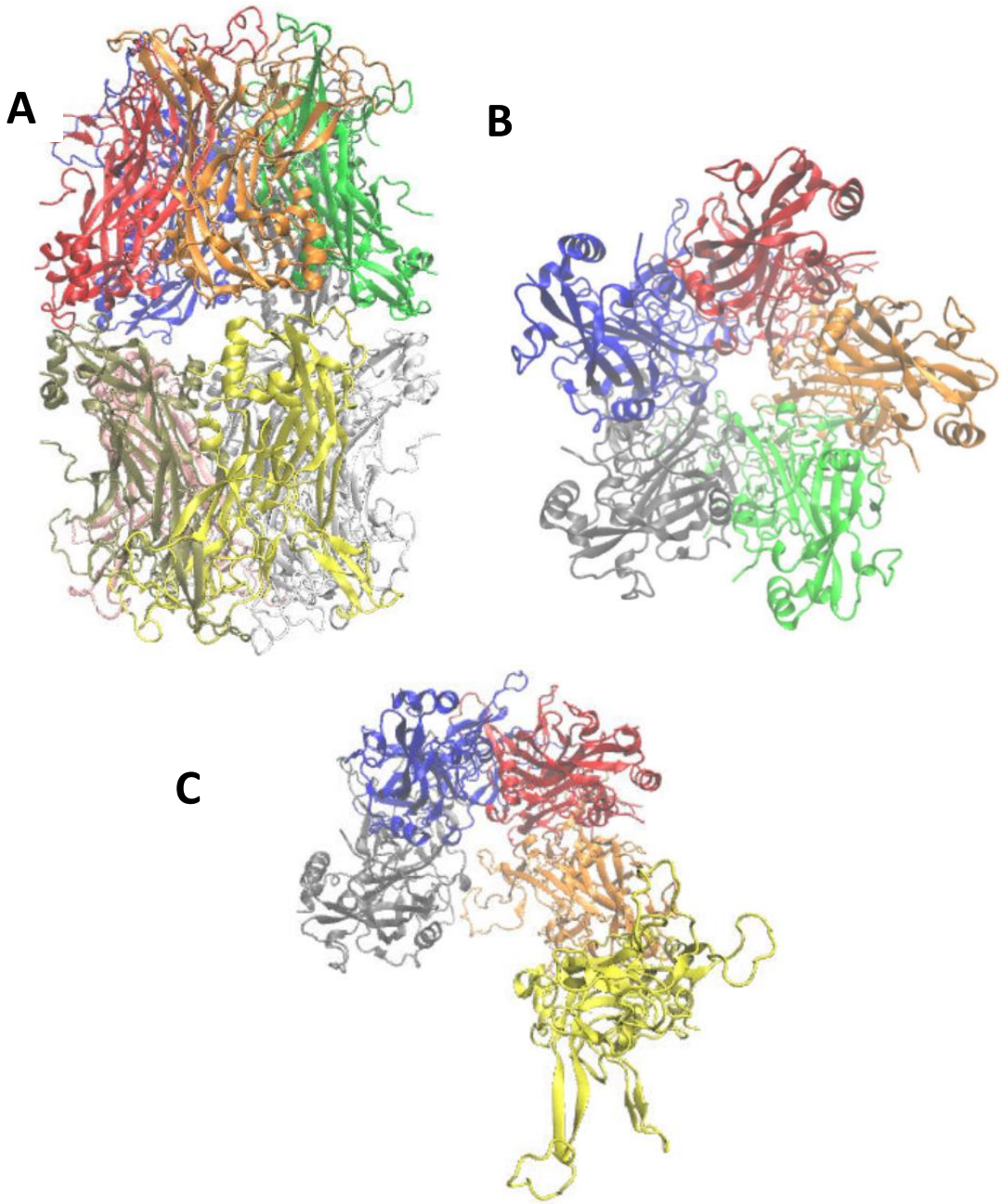

Figure 12. Crystal structure 6IGE of HPV 59 capsid L1 with chains A, B, C, D, E, F, G, H, I, and J, which was before [Figure 12.A] and after [Figure 12.B] using VMD to choose the only chains A, B, C, D, and H. If E was chosen instead of H the crystal structure would be like in [Figure 12.C].

CHAPTER IV

RESULTS

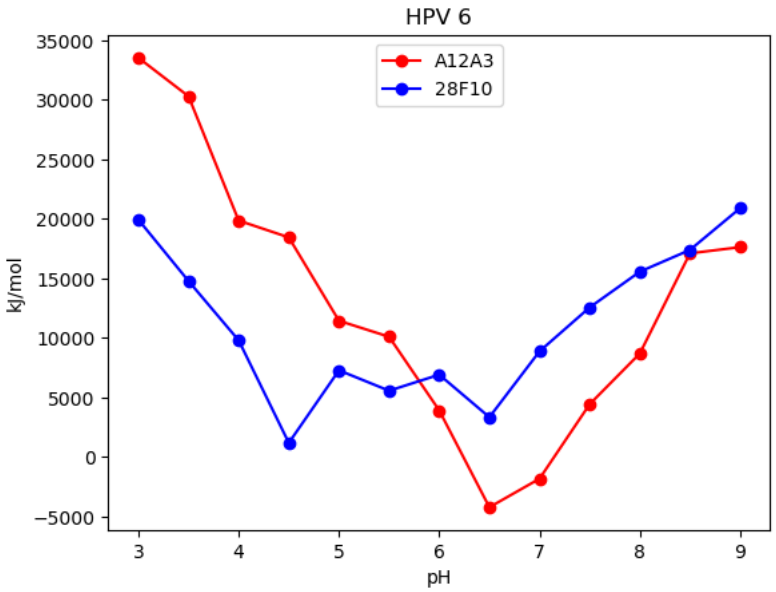

Figure 13. HPV 6 capsid-antibodies A12A3 and 28F10 binding energy vs pH level. This figure represents the binding energies ranging from -5000 to 35,000 kilojoules per mole (kJ/mol) across the pH values, which are determined into 3.0, 3.5, 4.0, 4.5, 5.0, 5.5, 6.0, 6.5, 7.0, 7.5, 8.0, 8.5, and 9.0.

The energy values of the antibody A12A3 decrease, reaching the lowest energy at pH 6.5 and then increase at higher pH levels. Unlike A12A3, the antibody 28F10 has the two lowest energies at pH 4.5 and 6.5 levels. The antibody A12A3 binds best to HPV 6 at higher pH levels. In the 28F10 antibody, at pH levels 4.5 and 6.5, it has relatively strong binding energies to the HPV 6 capsid. Comparing the two antibodies, HPV 6 prefers binding to 28F10, as shown by the low energies at 4.5 pH values for 28F10 compared to A12A3. This indicates that 28F10 is a suitable candidate for protecting against this variant at vaginal pH levels. Based on this evidence, the antibody 28F10 would provide better protection against this HPV 6 variant from genital warts (Figure 13).

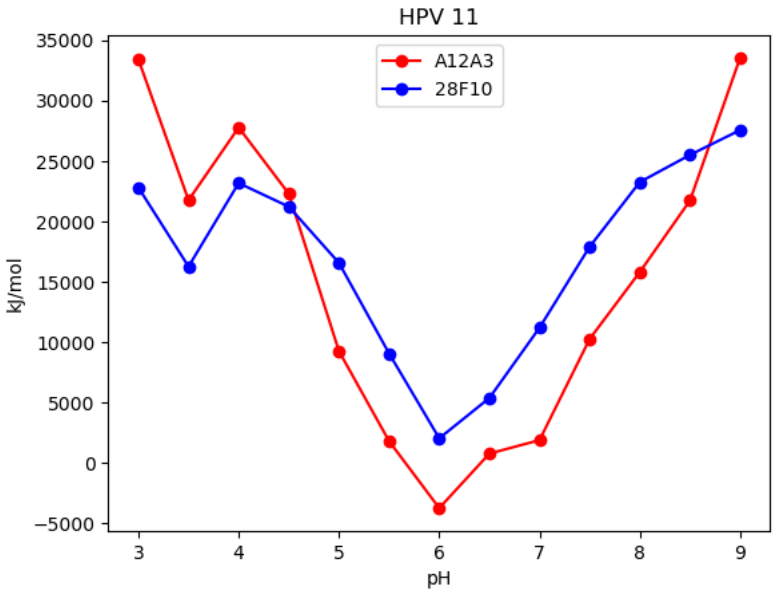

Figure 14. HPV 11 capsid-antibodies A12A3 and 28F10 binding energy vs pH level. This figure represents the binding energies ranging from -5000 to 35,000 kilojoules per mole (kJ/mol) across the pH values, which are determined into 3.0, 3.5, 4.0, 4.5, 5.0, 5.5, 6.0, 6.5, 7.0, 7.5, 8.0, 8.5, and 9.0.

The energies of both antibodies increase as the environment's pH becomes lower and higher from least value at pH 6.0. The graph represents the same pattern across both antibodies A12A3 and antibody 28F10 predicting binding best at the middle to this HPV 11 capsid. There is less preference for low-pH environments, so neither antibody is the best candidate for protecting from HPV 11 (Figure 14).

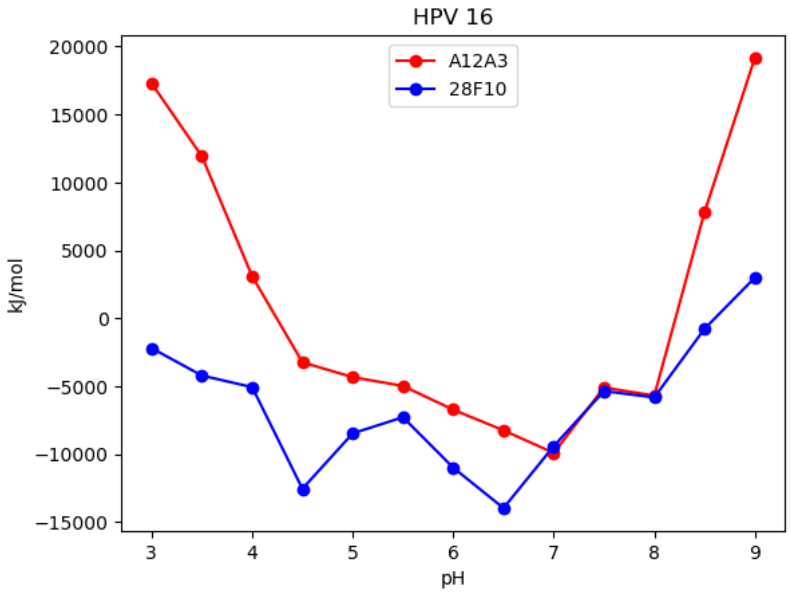

Figure 15. HPV 16 capsid-antibodies A12A3 and 28F10 binding energy vs pH level. This figure represents the binding energies ranging from -15,000 to 20,000 kilojoules per mole (kJ/mol) across the pH values, which are determined into 3.0, 3.5, 4.0, 4.5, 5.0, 5.5, 6.0, 6.5, 7.0, 7.5, 8.0, 8.5, and 9.0.

The energy values of the antibody A12A3 decrease, reaching the lowest energy at pH 7.0 then increasing at higher pH levels. Unlike A12A3, the antibody 28F10 has the two lowest energies at pH 4.5 and 6.5. The antibody A12A3 binds best to HPV 16 at higher pH levels. In the 28F10 antibody, at pH levels 4.5 and 6.5, it has relatively strong binding energies to the HPV 16 capsid. Comparing the two antibodies, the predicted binding energies for antibody A12A3 are generally higher than those for antibody 28F10 across all pH levels. However, there is a preference for binding to 28F10 as shown by the low energies at 4.5 and 6.5 pH for 28F10 compared to A12A3. This indicates that 28F10 is a suitable candidate for protecting against this variant at vaginal and cervical pH levels. Based on this evidence, the antibody 28F10 would provide better protection against this HPV 16 variant (Figure 15).

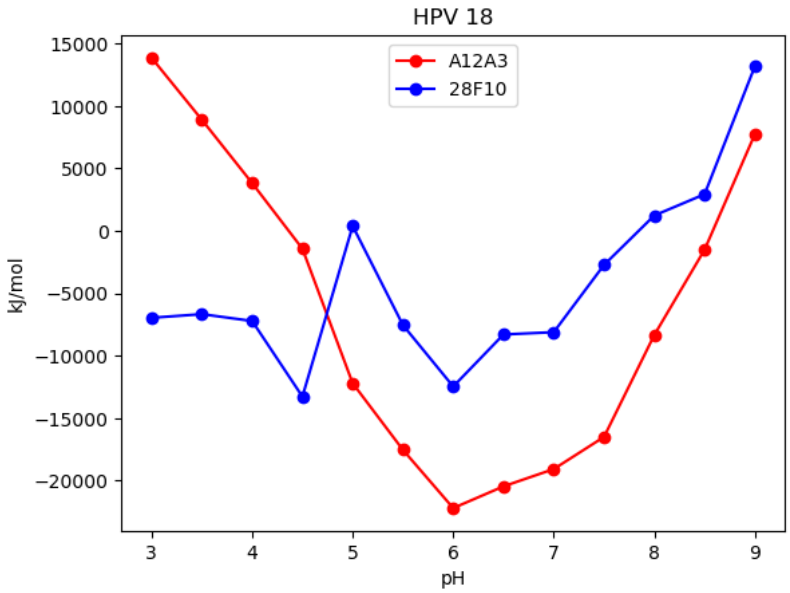

Figure 16. HPV 18 capsid-antibodies A12A3 and 28F10 binding energy vs pH level. This figure represents the binding energies ranging from -23,000 to 15,000 kilojoules per mole (kJ/mol) across the pH values, which are determined into 3.0, 3.5, 4.0, 4.5, 5.0, 5.5, 6.0, 6.5, 7.0, 7.5, 8.0, 8.5, and 9.0.

The energy values of the antibody A12A3 decrease, reaching the lowest energy at pH 6.0 then increasing at higher pH levels. Unlike A12A3, the antibody 28F10 has the two lowest energies at pH 4.5 and 6.0. The antibody A12A3 binds best to HPV 16 at higher pH levels. In the 28F10 antibody, at pH levels 4.5 and 6.0, it has relatively strong binding energies to the HPV 18 capsid. Comparing the two antibodies, there is a preference for binding to 28F10 as shown by the low energies at 4.5 and 6.0 pH for 28F10 compared to A12A3. This indicates that 28F10 is a suitable candidate for protecting against this variant at vaginal and cervical pH levels. Based on this evidence, the antibody 28F10 would provide better protection against this HPV 18 variant (Figure 16).

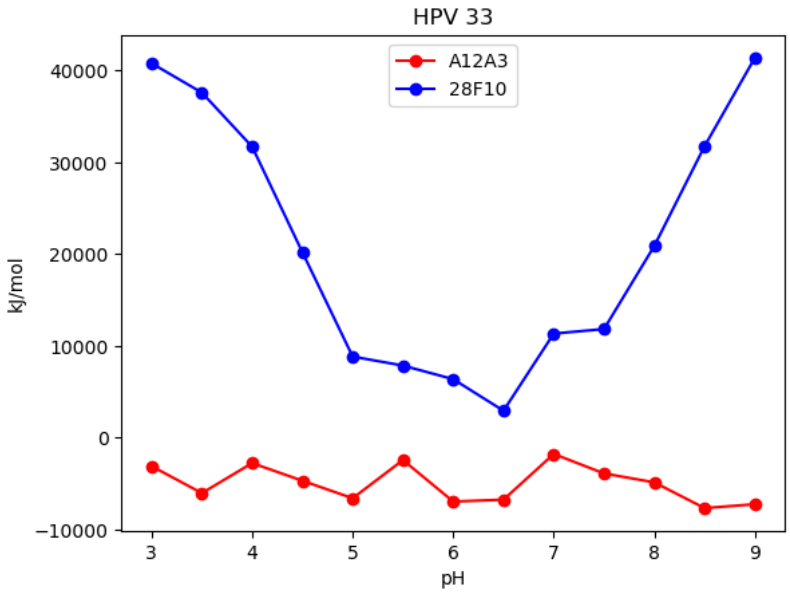

Figure 17. HPV 33 capsid-antibodies A12A3 and 28F10 binding energy vs pH level. This figure represents the binding energies ranging from -10,000 to 42,000 kilojoules per mole (kJ/mol) across the pH values, which are determined into 3.0, 3.5, 4.0, 4.5, 5.0, 5.5, 6.0, 6.5, 7.0, 7.5, 8.0, 8.5, and 9.0.

The binding energies values increase and decrease showing some fluctuations between the A12A3 antibody and the HPV virus. The energy values of the antibody 28F10 values decrease, reaching the lowest energy at pH 6.5 then increasing at higher pH levels. The antibody A12A3 does not bind best to HPV 33. The 28F10 antibody binds best at pH levels 6.5 and has relatively strong binding energies to the HPV 33 capsid. Comparing the two antibodies, the antibody 28F10 prefers binding to HPV 33 shown by the low energies at 6.5 pH values for 28F10 compared to A12A3. This indicates that 28F10 is a suitable candidate for protecting against this variant at cervical pH levels. Based on this evidence, the antibody 28F10 would provide better protection against this HPV 33 variant (Figure 17).

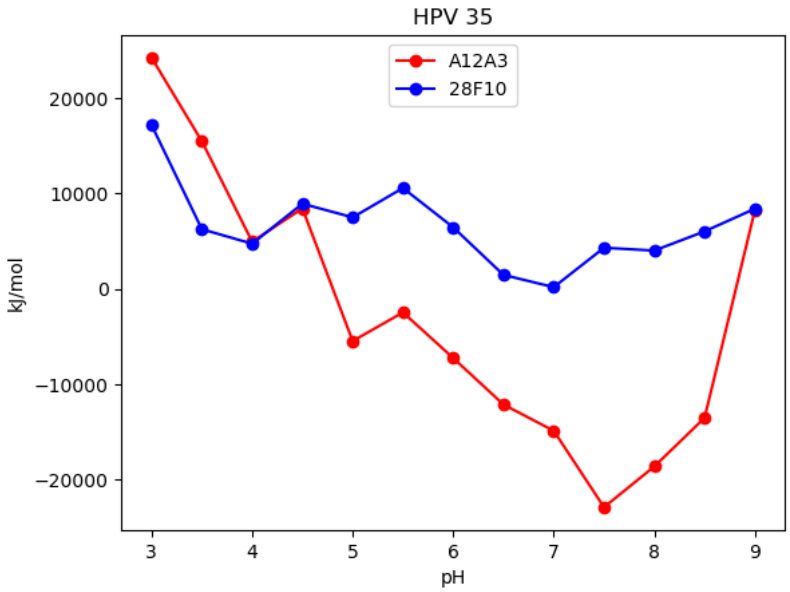

Figure 18. HPV 35 capsid-antibodies A12A3 and 28F10 binding energy vs pH level. This figure represents the binding energies ranging from -23,000 to 25,000 kilojoules per mole (kJ/mol) across the pH values, which are determined into 3.0, 3.5, 4.0, 4.5, 5.0, 5.5, 6.0, 6.5, 7.0, 7.5, 8.0, 8.5, and 9.0.

The energy values of the antibody A12A3 decrease, reaching the lowest energy at pH 7.5, then increasing at higher pH levels. The binding energies values increase and decrease showing some fluctuations between the 28F10 antibody and the HPV virus. The antibody A12A3 shows relatively strong binding energies to the HPV 35 capsid at 7.5. Also, the 28F10 antibody binds best at pH levels 7.0. Comparing the two antibodies, the antibody A12A3 prefers binding to HPV 35 as shown by the negative energy at 7.5 pH values for A12A3 compared to 28F10. This indicates that A12A3 is a suitable candidate for protecting against this variant at cervical pH levels. Based on this evidence, the antibody A12A3 would provide better protection against this HPV 35 variant (Figure 18).

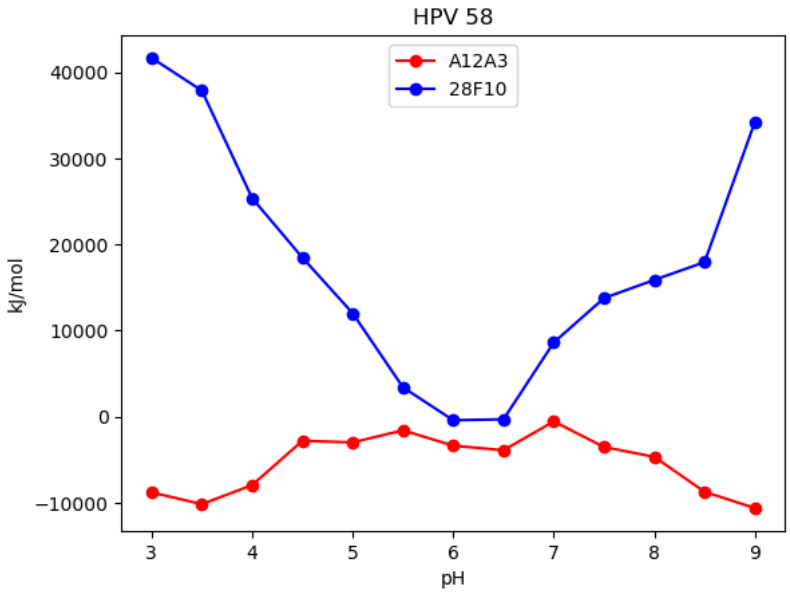

Figure 19. HPV 58 capsid-antibodies A12A3 and 28F10 binding energy vs pH level. This figure represents the binding energies ranging from -11,000 to 42,000 kilojoules per mole (kJ/mol) across the pH values, which are determined into 3.0, 3.5, 4.0, 4.5, 5.0, 5.5, 6.0, 6.5, 7.0, 7.5, 8.0, 8.5, and 9.0.

The binding energies values increase and decrease showing some fluctuations between the A12A3 antibody and the HPV virus. The energy values of the antibody 28F10 values decrease, reaching the lowest energy at pH 6.0 - 6.5, then increasing at higher pH levels. The antibody A12A3 does not bind best to HPV 58. The 28F10 antibody binds best at pH levels 6.0 - 6.5 and has relatively strong binding energies to HPV 58 capsid. Comparing the two antibodies, the antibody 28F10 prefers binding to HPV 58 shown by the low energies at 6.0 - 6.5 pH values for 28F10 compared to A12A3. This indicates that 28F10 is a suitable candidate for protecting against this variant at cervical pH levels. Based on this evidence, the antibody 28F10 would provide better protection against this HPV 58 variant (Figure 19).

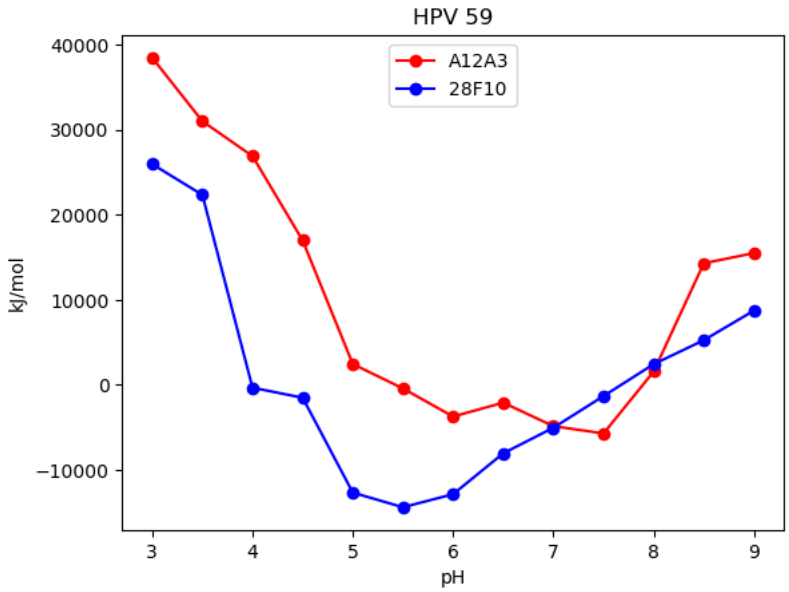

Figure 20. HPV 59 capsid-antibodies A12A3 and 28F10 binding energy vs pH level. This figure represents the binding energies ranging from -15,000 to 40,000 kilojoules per mole (kJ/mol) across the pH values, which are determined into 3.0, 3.5, 4.0, 4.5, 5.0, 5.5, 6.0, 6.5, 7.0, 7.5, 8.0, 8.5, and 9.0.

The energy values of the antibody A12A3 decrease, reaching the lowest energy at pH 7.5 then increasing at higher pH levels. Unlike A12A3, the antibody 28F10 has the lowest energy at pH 5.5 level. The antibody A12A3 binds best to HPV 59 at higher pH levels. The antibody 28F10 has relatively strong binding energies to HPV 59 capsid at pH 5.5 level. Comparing the two antibodies, the antibody A12A3 prefers binding to HPV 59 shown by the low energies at pH cervical levels specifically at 7.5 pH value for A12A3 compared to 28F10. This indicates that A12A3 is a suitable candidate for protecting against this variant at cervical pH levels. Based on this evidence, the antibody A12A3 would provide better protection against this HPV 59 variant (Figure 20).

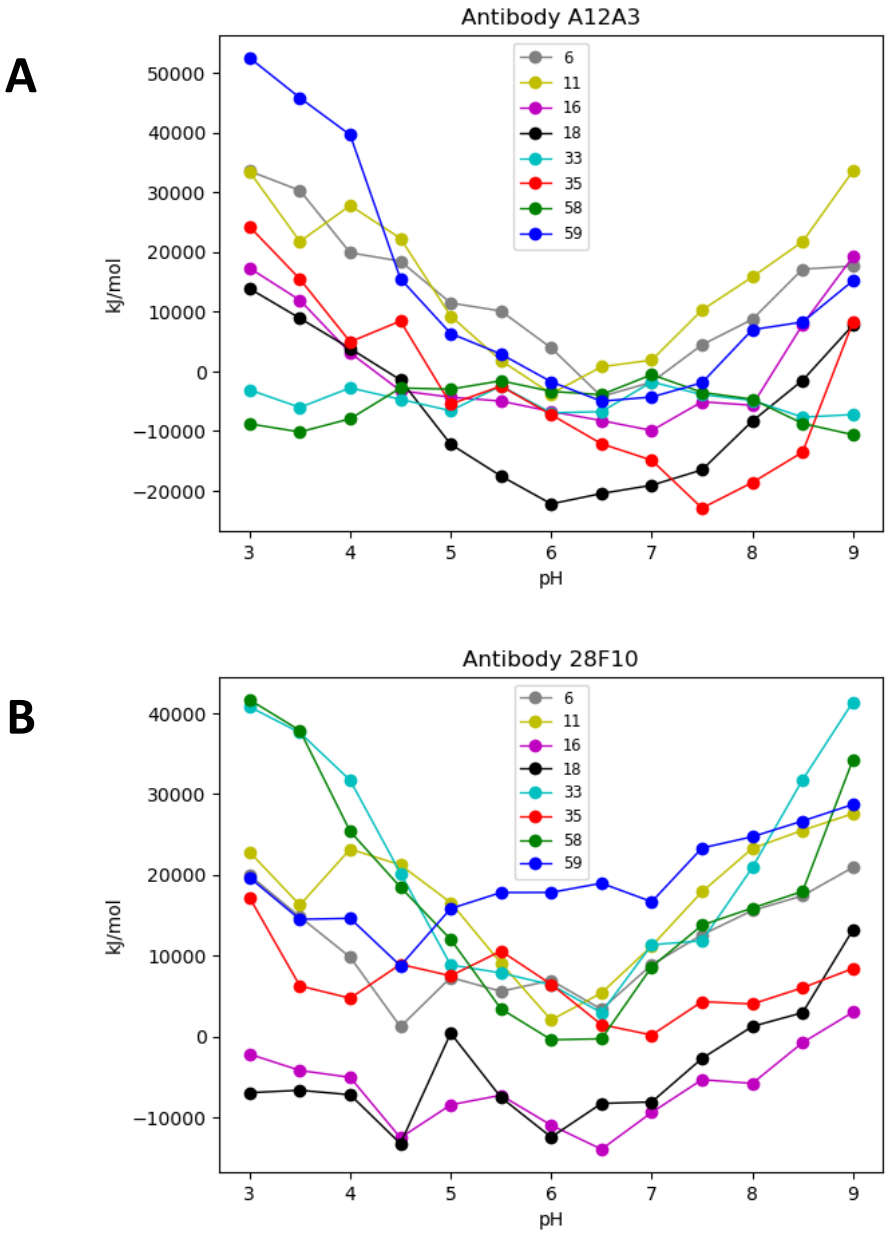

Figure 21. The antibody A12A3 (A) and 28F10 (B) binding energy to all capsid of HPVs vs pH level. This figure represents the binding energies across the pH values, which are determined into 3.0, 3.5, 4.0, 4.5, 5.0, 5.5, 6.0, 6.5, 7.0, 7.5, 8.0, 8.5, and 9.0.

The binding energy of all HPV's capsid to the antibody A12A3 has shown strongly for HPV 35 and 59 Figure (21.A). On the other hand, the antibody 28F10 shows a strong binding energy to HPV 6, 16, 18, 33, and 58.

CHAPTER V

DISCUSSION AND FUTURE WORK

In this thesis, a computational pipeline was applied to predict the binding energies of two antibodies, the antibody A12A3 and the antibody 28F10, interacting with the capsid proteins of different HPV types: 6, 11, 16, 18, 33, 35, 58, and 59. Antibody A12A3 showed strong binding energy and favorable interactions with HPV types 35 and 59, suggesting it is a preferable candidate for these specific HPV strains. On the other hand, antibody 28F10 represented strong binding energy and interactions with HPV types 6, 16, 18, 33, and 58, indicating its effectiveness against these strains. Moreover, this work provided predictions that both antibody A12A3 and antibody 28F10 have a good protection against those HPV types from cervical cancer or genital warts. Furthermore, this thesis highlights the importance of computational approaches in understanding antibody-capsid of HPV interactions and their pH-dependence, providing valuable insights into the development of effective antibodies against specific HPV strains.

Future Work

Experiments could be performed in the laboratory to validate some of the results with the interactions across pH levels. Also, new computational studies or pipelines may be applied to these capsid proteins of HPV and the antibodies. On the other hand, applying this pipeline to other HPV proteins like E6 and E7 and predicting the binding energy between them and the antibodies A12A3 and 28F10 is another potential research direction. Furthermore, exploring the results of this thesis in more detail is another research direction by conducting studies of relationships with the other cancers and comparing the antibodies with pH for their locations such as anal, penile, and oropharyngeal cancers.

BIBLIOGRAPHY

[1] Centers for Disease Control and Prevention. 2022. Std Facts - Human papillomavirus (HPV). (April 2022). Retrieved March 31, 2023 from https://www.cdc.gov/std/hpv/stdfact-hpv.htm

[2] De Sanjosé, S., Brotons, M. and Pavón, M.A. 2018. The natural history of human papillomavirus infection. *Best Practice & Research Clinical Obstetrics & Gynaecology*. 47, (Feb. 2018), 2–13. DOI:https://doi.org/10.1016/j.bpobgyn.2017.08.015.

[3] IARC Working Group on the Evaluation of Carcinogenic Risks to Humans. Human papillomaviruses. Lyon (FR): International agency for research on cancer; 2007. (IARC Monographs on the evaluation of carcinogenic risks to humans, No. 90.) 1, Human papillomavirus (HPV) infection. Available from: https://www.ncbi.nlm.nih.gov/books/NBK321770/

[4] Centers for Disease Control and Prevention. 2022. What should I know about cervical cancer screening? (December 2022). Retrieved March 31, 2023 from https://www.cdc.gov/cancer/cervical/basic_info/screening.htm

[5] Waller, J., McCaffery, K., Nazroo, J. and Wardle, J. 2005. Making sense of information about HPV in cervical screening: a qualitative study. *British Journal of Cancer*. 92, 2 (Jan. 2005), 265–270. DOI:https://doi.org/10.1038/sj.bjc.6602312.

[6] Centers for Disease Control and Prevention. 2021. HPV treatment. (July 2021). Retrieved March 31, 2023 from https://www.cdc.gov/std/hpv/treatment.htm

[7] Centers for Disease Control and Prevention. 2021. Human papillomavirus (HPV) infection - STI treatment guidelines. (July 2021). Retrieved March 31, 2023 from https://www.cdc.gov/std/treatment-guidelines/anogenital-warts.htm

[8] Centers for Disease Control and Prevention. 2022. How is cervical cancer diagnosed and treated? (December 2022). Retrieved March 31, 2023 from https://www.cdc.gov/cancer/cervical/basic_info/diagnosis_treatment.htm

[9] Centers for Disease Control and Prevention. 2021. Epidemiology and prevention of vaccine-preventable diseases: Human papillomavirus. (August 2021). Retrieved March 31, 2023 from https://www.cdc.gov/vaccines/pubs/pinkbook/hpv.html

[10] Center for Biologics Evaluation and Research. October 16, 2009 approval letter - Cervarix. Retrieved March 31, 2023 from https://web.archive.org/web/20091019061945/https:/www.fda.gov/BiologicsBloodVaccines/Vaccines/ApprovedProducts/ucm186959.htm

[11] Deschuyteneer, M., Elouahabi, A., Plainchamp, D., Plisnier, M., Soete, D., Corazza, Y., Lockman, L., Giannini, S. and Deschamps, M. 2010. Molecular and structural characterization of the L1 virus-like particles that are used as vaccine antigens in *Cervarix* ™, the AS04-adjuvanted HPV-16 and -18 cervical cancer vaccine. *Human Vaccines*. 6, 5 (May 2010), 407–419. DOI:https://doi.org/10.4161/hv.6.5.11023.

[12] FDA. Cervarix. Retrieved March 31, 2023 from https://www.fda.gov/vaccines-blood-biologics/vaccines/cervarix

[13] FDA. 2021. Package Insert: Gardasil. Retrieved March 31, 2023 from https://www.fda.gov/files/vaccines,%20blood%20&%20biologics/published/Package-Insert---Gardasil.pdf.

[14] Drugs.com. Gardasil 9 (human papillomavirus 9-valent vaccine, recombinant) FDA approval history. Retrieved March 31, 2023 from https://www.drugs.com/history/gardasil-9.html

[15] FDA. Gardasil 9. Retrieved March 31, 2023 from https://www.fda.gov/vaccines-blood-biologics/vaccines/gardasil-9

[16] Centers for Disease Control and Prevention. 2022. Vaccine information statement: Recent and upcoming changes. (November 2022). Retrieved March 31, 2023 from https://www.cdc.gov/vaccines/hcp/vis/what-is-new.html

[17] Horvath, C.A., Boulet, G.A., Renoux, V.M., Delvenne, P.O. and Bogers, J.-P.J. 2010. Mechanisms of cell entry by human papillomaviruses: an overview. *Virology Journal*. 7, 1 (Dec. 2010), 11. DOI:https://doi.org/10.1186/1743-422X-7-11.

[18] Kirnbauer, R., Booy, F., Cheng, N., Lowy, D.R. and Schiller, J.T. 1992. Papillomavirus L1 major capsid protein self-assembles into virus-like particles that are highly immunogenic. *Proceedings of the National Academy of Sciences*. 89, 24 (Dec. 1992), 12180–12184. DOI:https://doi.org/10.1073/pnas.89.24.12180.

[19] Akuzum, B., Kim, S., Nguyen, T.T., Hong, J., Lee, S., Kim, E., Kim, J., Choi, Y., Jhun, H., Lee, Y., Kim, H., Sohn, D.H. and Kim, S. 2018. L1 Recombinant Proteins of HPV Tested for Antibody Forming Using Sera of HPV Quadrivalent Vaccine. Immune Network. 18, 3 (2018), e19. DOI:https://doi.org/10.4110/in.2018.18.e19.

[20] Tumban, E., Peabody, J., Peabody, D.S. and Chackerian, B. 2013. A universal virus-like particle-based vaccine for human papillomavirus: Longevity of protection and role of endogenous and exogenous adjuvants. *Vaccine*. 31, 41 (Sep. 2013), 4647–4654. DOI:https://doi.org/10.1016/j.vaccine.2013.07.052.

[21] Humphrey, W., Dalke, A. and Schulten, K. 1996. VMD: Visual molecular dynamics. *Journal of Molecular Graphics*. 14, 1 (Feb. 1996), 33–38. DOI:https://doi.org/10.1016/0263-7855(96)00018-5.

[22] Eswar, N., Webb, B., Marti-Renom, M.A., Madhusudhan, M.S., Eramian, D., Shen, M., Pieper, U. and Sali, A. 2006. Comparative Protein Structure Modeling Using Modeller. *Current Protocols in Bioinformatics*. 15, 1 (Sep. 2006). DOI:https://doi.org/10.1002/0471250953.bi0506s15.

[23] Farrell, D.W., Speranskiy, K. and Thorpe, M.F. 2010. Generating stereochemically acceptable protein pathways. Proteins: Structure, Function, and Bioinformatics. 78, 14 (Nov. 2010), 2908–2921. DOI:https://doi.org/10.1002/prot.22810.

[24] Dolinsky, T.J., Czodrowski, P., Li, H., Nielsen, J.E., Jensen, J.H., Klebe, G. and Baker, N.A. 2007. PDB2PQR: expanding and upgrading automated preparation of biomolecular structures for molecular simulations. *Nucleic Acids Research*. 35, Web Server (May 2007), W522–W525. DOI:https://doi.org/10.1093/nar/gkm276.

[25] Dolinsky, T.J., Nielsen, J.E., McCammon, J.A. and Baker, N.A. 2004. PDB2PQR: an automated pipeline for the setup of Poisson-Boltzmann electrostatics calculations. *Nucleic Acids Research*. 32, Web Server (Jul. 2004), W665–W667. DOI:https://doi.org/10.1093/nar/gkh381.

[26] Baker, N.A., Sept, D., Joseph, S., Holst, M.J. and McCammon, J.A. 2001. Electrostatics of nanosystems: Application to microtubules and the ribosome. *Proceedings of the National Academy of Sciences*. 98, 18 (Aug. 2001), 10037–10041. DOI:https://doi.org/10.1073/pnas.181342398.

[27] Li, Z. et al. 2017. Crystal Structures of Two Immune Complexes Identify Determinants for Viral Infectivity and Type-Specific Neutralization of Human Papillomavirus. *mBio*. 8, 5 (Nov. 2017), e00787-17. DOI:https://doi.org/10.1128/mBio.00787-17.

[28] Berman, H.M. 2000. The Protein Data Bank. *Nucleic Acids Research*. 28, 1 (Jan. 2000), 235–242. DOI:https://doi.org/10.1093/nar/28.1.235. https://www.rcsb.org/

[29] Bishop, B., Dasgupta, J., Klein, M., Garcea, R.L., Christensen, N.D., Zhao, R. and Chen, X.S. 2007. Crystal Structures of Four Types of Human Papillomavirus

L1 Capsid Proteins. *Journal of Biological Chemistry*. 282, 43 (Oct. 2007), 31803–31811. DOI:https://doi.org/10.1074/jbc.M706380200.

[30] Li, Z. et al. 2018. Rational design of a triple-type human papillomavirus vaccine by compromising viral-type specificity. *Nature Communications*. 9, 1 (Dec. 2018), 5360. DOI:https://doi.org/10.1038/s41467-018-07199-6.

[31] Li, Z. et al. 2016. The C-Terminal Arm of the Human Papillomavirus Major Capsid Protein Is Immunogenic and Involved in Virus-Host Interaction. Structure. 24, 6 (Jun. 2016), 874–885. DOI:https://doi.org/10.1016/j.str.2016.04.008.

[32] Van Rossum, G. 1995. Python reference manual. Department of computer science [CS]. CWI.

[33] Hunter, J.D. 2007. Matplotlib: A 2D Graphics Environment. *Computing in Science & Engineering*. 9, 3 (2007), 90–95. DOI:https://doi.org/10.1109/MCSE.2007.55.

[34] Centers for Disease Control and Prevention. 2022. Cancers caused by HPV. (February 2022). Retrieved March 31, 2023 from https://www.cdc.gov/hpv/parents/cancer.html

[35] David Pride. 2020. Viruses can help us as well as harm us. (December 2020). Retrieved March 31, 2023 from https://www.scientificamerican.com/article/viruses-can-help-us-as-well-as-harm-us/

[36] Centers for Disease Control and Prevention. 2021. HPV vaccination: What everyone should know. (November 2021). Retrieved March 31, 2023 from https://www.cdc.gov/vaccines/vpd/hpv/public/index.html

[37] Xing, S., Wallmeroth, N., Berendzen, K.W. and Grefen, C. 2016. Techniques for the analysis of protein-protein interactions in vivo. *Plant Physiology*. (Apr. 2016), pp.00470.2016. DOI:https://doi.org/10.1104/pp.16.00470.

[38] Zahiri, J., Bozorgmehr, J. and Masoudi-Nejad, A. 2013. Computational Prediction of Protein–Protein Interaction Networks: Algorithms and Resources. *Current Genomics*. 14, 6 (Sep. 2013), 397–414. DOI:https://doi.org/10.2174/1389202911314060004.

[39] Rao, V.S., Srinivas, K., Sujini, G.N. and Kumar, G.N.S. 2014. Protein-Protein Interaction Detection: Methods and Analysis. *International Journal of Proteomics*. 2014, (Feb. 2014), 1–12. DOI:https://doi.org/10.1155/2014/147648.

[40] Sunita, Sajid, A., Singh, Y. and Shukla, P. 2020. Computational tools for modern vaccine development. *Human Vaccines & Immunotherapeutics*. 16, 3 (Mar. 2020), 723–735. DOI:https://doi.org/10.1080/21645515.2019.1670035.

[41] Lykke, M.R., Becher, N., Haahr, T., Boedtkjer, E., Jensen, J.S. and Uldbjerg, N. 2021. Vaginal, Cervical and Uterine pH in Women with Normal and Abnormal Vaginal Microbiota. *Pathogens*. 10, 2 (Jan. 2021), 90. DOI:https://doi.org/10.3390/pathogens10020090.

[42] Liu, X. et al. 2019. Neutralization sites of human papillomavirus-6 relate to virus attachment and entry phase in viral infection. *Emerging Microbes & Infections*. 8, 1 (Jan. 2019), 1721–1733. DOI:https://doi.org/10.1080/22221751.2019.1694396.